

Multi-wavelength study of a flare and burst associated coronal mass ejection

S Prasanna Subramanian^{a*}, G Selvarani^b & A Shanmugaraju^c

^aRadio Astronomy Centre, Ooty 654 001, India

^bSri Meenakshi Govt. Arts College for Women, Madurai 625 002, India

^cArul Anandar College, Madurai 625 514, India

Received 21 January 2016; revised 29 March 2017; accepted 05 July 2017

The present study consists of the radio emissions observed on 15 May 2013 by ground based and space based radio observations. An intensive solar X-ray flare from the location N12E64 was associated with a halo coronal mass ejection (CME) of speed 1366 km/s observed in white light by Solar and Heliospheric Observatory (SOHO)/Large Angle Spectrometric Coronagraph (LASCO) coronagraph. Metric type II and IV radio emission were detected by Culgoora and Bruny island radio spectrograph (BIRS) after flare onset. Also, decameter-hectometric (DH) type II radio burst was detected by wind/radio and plasma wave experiment (WAVES). The low frequency radio signature was found to be generated between 8-42 Ro (Ro= one solar radius). From the analysis, both the high and low frequency type II radio signatures seem to be generated due to shock driven by the CME. This CME was also associated with SEP, IP shock and geomagnetic storm.

Keywords: Sun, Solar flare, Coronal mass ejection, Radio bursts

1 Introduction

Type II radio burst, observed as a slowly drifting signature in the radio dynamic spectrum, is an important tool to understand the physical phenomena of shock in the solar corona and in the interplanetary (IP) medium. They are known to be electrons generated from shock waves that radiate as local plasma frequency and its harmonic. Metric type II bursts generally appear between the frequency range 20 MHz - 100 MHz and that are caused by electrons accelerated from the shocks travelling through lower solar corona. They can be detected by solar radio spectrogram at ground based detection. Other type II bursts (DH and km) in the dynamic spectrum at low frequency that are generated by shocks travelling through upper solar corona and IP space. They can be detected by spacecraft detection between the frequency range 16 MHz to few kHz.

CMEs are often associated with type II radio bursts that are also indicators of coronal and interplanetary shocks. Generally, fast CMEs (>1000 km/s) are in association with m-to-km (metric to kilometric) type II bursts. Gopalswamy *et al.*¹ found that CME associated with m-to-km type II bursts were more energetic than the CMEs associated with DH type II bursts. They also found (i) most of m-to-km type II

burst events were associated with intensive flares (>M5.0 X-ray class), and (ii) about 78 % of m-to-km type II were associated with major solar energetic particle (SEP) events.

Investigation on the association of CMEs with radio bursts and/or flares have been done by several authors²⁻⁹. CMEs are also found to be associated with solar energetic particle events and geo-magnetic storms⁹⁻¹¹. Klein *et al.*¹² studied a metric type II event on 27 November 1997. They found close association between solar X-ray flares (hard and soft) and metric type II burst, i.e., features in frequency range from 411 MHz to 40 MHz was found to be due to the solar flare. Gopalswamy *et al.*¹³ found that most of the metric type II radio burst's onset occurred below 1.5 Ro. Some time, metric type IV occurs before or after type II emission. The aim of the present study is to find out (i) where in the corona and interplanetary medium the radio bursts were generated in this event and what are the Alfvénic condition to generate shocks, and (ii) what are the other associated activities related to this event. The first step is studied using the known electron density model¹⁴. Ground and spacecraft data associated with this event are utilized for studying the second step.

2 Data Selection

White light observations obtained by Large Angle Solar Coronagraph (LASCO) on Solar and Heliospheric

*Corresponding author (E-mail: jprasannasunn@gmail.com)

Observatory (SOHO) mission are taken from the website www.cdaw.gsfc.nasa.gov¹⁵. Data regarding the radio spectrum in the metric wavelength range of radio bursts is provided by Culgoora and BIRS spectrograph, Australia. Radio observations in the DH range, obtained by radio and plasma wave experiment on board the wind spacecraft, are listed in the online catalogue. The X-ray flare data is considered from flare website www.noaa.ngdc.gov¹⁶ maintained by National Oceanographic Atmospheric Administration (NOAA) of National Aeronautics and Space Administration (NASA). Data corresponding to SEPs are taken from the online catalogue www.umbra.nascom.nasa.gov/sep¹⁷. Coronal shock speed is estimated using the shock signatures seen in Solar Terrestrial Relations Observatory (STEREO)/COR1 coronagraph's images. The IP shock data observed by wind spacecraft is considered from the web <http://omniweb.gsfc.nasa.gov/cgi/nx1.cgi>. The geomagnetic disturbance storm index (Dst) was obtained from online catalogue <http://wdc.kugi.kyoto-u.ac.jp/dst/dir/> and it has been maintained by the Center for Geomagnetism, Kyoto University, Japan. Table 1 gives the details of radio emissions associated with the present event (radio bursts, frequency, time and spectrograph) and the flare and CME details are given in Table 2. The properties derived from the bursts (like frequency range, drift rate, shock speed and shock distance range) are given in Table 3.

The Alfven speed is found using the following relation:

$$V_A = 2 \times 10^6 B / \sqrt{\rho} \quad \dots (1)$$

The electron density (ρ) is determined by the plasma frequency equation, $f = 9\sqrt{\rho}$. The Alfven speed is estimated for the plasma frequency using Leblanc, Dulk and Bougeret¹⁸ model,

#	Radio burst	Start frequency	End frequency	Time	Spectrograph
1	Type IV	1300 MHz	570 MHz	01:32 UT – 01:42 UT	Culgoora
2	Type II *	~32 MHz	~20 MHz	01:48 UT – 01:57 UT	Culgoora
3	Type II *	~32 MHz	~20 MHz	01:48 UT – 01:57 UT	BIRS
4	Type II	1.5 MHz	250 kHz	04:30 UT – 07:30 UT	Wind/WAVES

(* - fundamental component of Type II burst)

$$\rho(r) = 3.3 \times 10^5 r^{-2} + 4.1 \times 10^6 r^{-4} + 8.0 \times 10^7 r^{-6} \quad \dots (2)$$

The magnetic field of the shock at various height is estimated using the magnetic field model by Dulk and McLean¹⁸.

$$B = 0.5(r-1)^{-1.5} \quad \dots (3)$$

The solar wind speed is considered from Sheeley *et al.*¹⁹

$$V_{sw} = 1.75 \times 10^5 \left[1 - e^{\frac{-(R-4.5)}{15.2}} \right] \quad \dots (4)$$

The aim of the study is to know, what are the radio emission associated with the CME and what is the role of shock parameters (Alfven speed, magnetic field, solar wind speed) between 1.5 Ro – 42 Ro during the propagation in the interplanetary medium.

#	Properties	Details
1	CME associated flare location/ Active Region	N12E64/AR 11748
2	GOES X-ray flare class	X1.2
3	LASCO CME Date time	15 May 2013 & 01:38 UT
4	LASCO CME speed	1366 km/s
5	LASCO CME width	360 degrees
6	LASCO CME range [C2, C3]	3-24 Ro
7	STEREO-B CME speed ^a [COR1, COR2]	1940 km/s
8	STEREO-B CME range [COR1, COR2, HI-1]	~2-87 Ro

a-SEEDS STEREO catalog

Property	High frequency Type II	Low frequency Type II
Frequency range	32 MHz – 7 MHz	1.5 MHz – 250 kHz
Duration	01:48 UT – 02:05 UT	04:30 UT – 07:30 UT
Drift rate	24.5 kHz/s	0.115 kHz/s
Density model Shock speed	1497 km/s	1300 km/s
Observed shock speed [STEREO]	1296 km/s	2063 km/s
Observed shock range	1.3 Ro – 3.2 Ro	24 Ro – 56 Ro
Density model Shock range	1.5 Ro – 2.6 Ro	8 Ro – 42 Ro
Density model	3 fold Saito <i>et al.</i> ²²	2 fold Leblanc <i>et al.</i> ¹⁴

3 Results and Discussion

First, an X class flare was detected by GOES at the location N12E64 at 01:25 UT on 15 May 2013 and it is shown in Fig. 1 (right panel). The rise time and duration of the flare are found to be 23 min and 33 min, respectively. Then, a halo CME was first observed by LASCO C2 coronagraph at 01:48 UT at 2.62 Ro (shown in Fig. 1-left panel). The speed and acceleration of CME were reported as 1366 km/s and -52.1 m/s^2 , respectively. The same CME was observed by the C3 coronagraph at 02:18 UT at a height of 7.2 Ro and final observed distance (FOD) of the CME was reported as 23 Ro. Using STEREO COR 1&2 coronagraph images (Fig. 2), the shock speed is obtained to be 1569 km/s during the period 01:48 UT – 02:05 UT between 1.3 Ro – 3.2 Ro distance ranges. The acceleration of the shock is found to be high after $\sim 4 \text{ Ro}$.

3.1 High frequency radio bursts

As given in Fig. 3a, Culgoora radio dynamic spectrum in the metric frequency range shows type IV and type II radio bursts associated with the CME. The spectrum reveals that type IV starts at a high frequency $\sim 1350 \text{ MHz}$ at 01:27 UT close to the start of an X-ray flare (01:25 UT). The radio emission continues up to $\sim 600 \text{ MHz}$. This type of radio emission is caused by fast electrons trapped in a post flare loop system emitting synchrotron radiation¹⁶. The electrons are supposed to be ejected from the flare reconnection site at the pre-phase of the CME. The time of occurrence of type IV around the start of flare is consistent with this. As seen in dynamic spectrum, the metric type II radio burst with fundamental and harmonic bands is visible below 60 MHz around 01:50 UT during the flare maximum.

Figure 3b shows the same metric type II, but it is clear with fundamental and harmonic band structures.

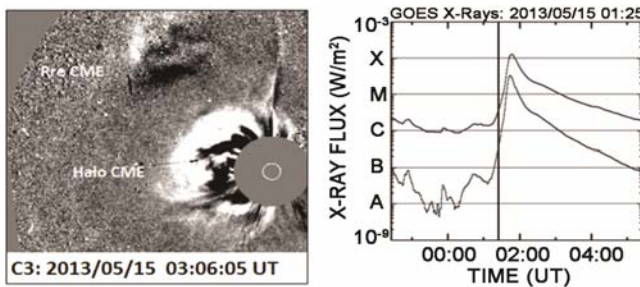


Fig. 1 — CME observed on 2013 May 15 observed by SOHO/LASCO –C3 coronagraph at 03:06 UT (left panel). GOES X-ray flare profile of the flare associated halo CME event (right panel). The peak intensity of the event is shown as X1.2 at 1-8 Å wavelength channel. The vertical line shows the time of observation 01:25 UT

The metric type II was detected by the BIRS (Bruny Island Radio Spectrometer) spectrograph. The BIRS is capable of detecting solar radio waves between 5 MHz to 65 MHz. The fundamental features are visible in the frequency range $\sim 32 \text{ MHz} - 20 \text{ MHz}$ during 01:48 UT – 01:57 UT. The BIRS intensity light curve shows an increase in radio intensity during the flare decay phase during which the spectrograph image shows an intense metric type II with fundamental and harmonic structure.

The continuation of the metric type II was also seen in the Deca-Hecta metric range in the Wind/WAVES spectrum as shown in Fig. 4. The extension of fundamental feature occurred in the range 16 MHz– 7 MHz during $\sim 01:55 \text{ UT} - 2:05 \text{ UT}$. Hence, the total frequency range of the fundamental

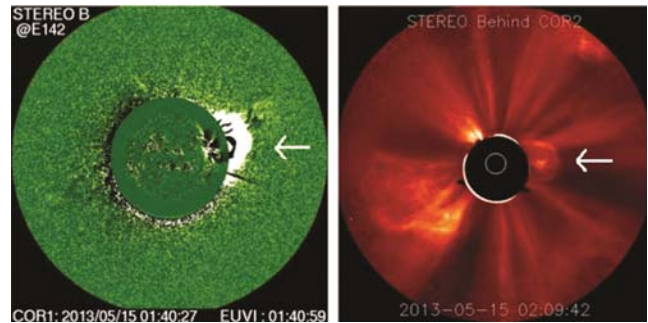


Fig. 2 — CME observed on 2013 May 15 as observed by STEREO/COR1 coronagraph (left panel) and STEREO/COR2 (right panel)

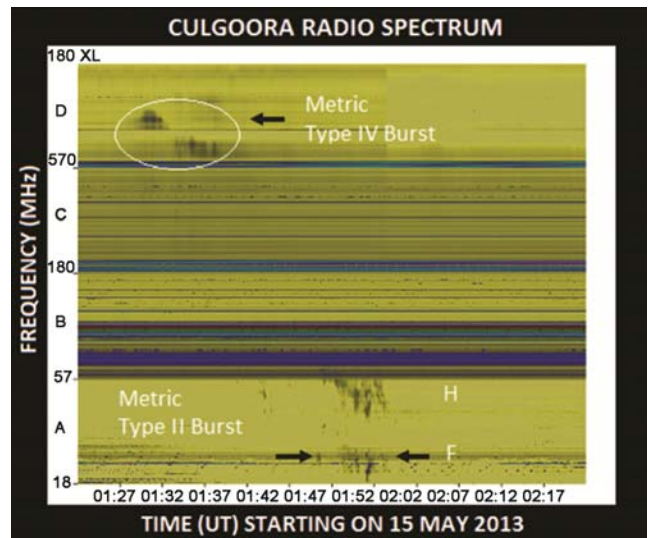


Fig. 3a — Type II burst is shown in the dynamic spectrum recorded by Culgoora spectrograph on 15 May 2013 between the frequency range 32 MHz – 20 MHz. Fundamental and harmonic bands of type II burst are noted as F and H during 01:50 UT – 01:57 UT. Metric type IV radio burst in the high frequency range 1300 MHz – 570 MHz is marked with an ellipse

structure ~ 32 MHz – 7 MHz during 01:48 UT – 02:05 UT as evidenced from Figs 4. Cane and Ericson¹⁷ studied a metric type II event on 01 November 2001 and they found that the fundamental range of frequency was 300 MHz – 10 MHz. They used combination of data from Culgoora, BIRS and Wind/WAVES spectrographs for that event.

Also, Gopalswamy and Kaiser⁴ studied the metric type II event on 1997 May 12 and they found that fundamental frequency band was in the range 60 MHz – 10 MHz similar to the present event. They found that the coronal shock generation was between the distance 1.5 R_o to 2.85 R_o . They used 3 fold Saito *et al.*²² model to estimate the shock range. Similar to this, in the present study, the coronal type II features were in metric and DH frequency (32 MHz – 7 MHz). The drift rate (df/dt) for this frequency range is found to be 24.5 kHz/s. According to the 3 fold Saito *et al.*²² density model, the present study suggests that the coronal type II burst might be generated from ~ 2.3 R_o to a maximum distance of around 4.5 R_o . The shock speed is found using above density model to be 1497 km/s. Note that the speed is the above the Alfvén speed (~ 800 km/s) between the distance 3 R_o – 4 R_o as shown in Fig. 6 and for a shock, it is able condition to travel through the corona to produce a type II radio burst⁴. While, the absence of frequency is found in dynamic spectrum between the range 6 MHz – 2 MHz. It suggests that the shock generation may be from the flank region of the CME

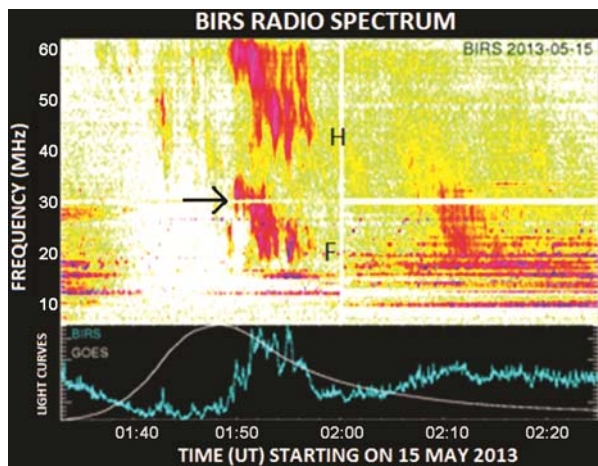


Fig. 3b — Metric type II burst as observed in the BIRS radio spectrum in the metric frequency range 60 MHz – 20 MHz. Fundamental and harmonic bands of type II burst are marked as F and H, respectively during $\sim 01:48$ UT – $01:57$ UT. At the bottom, X-ray flare profile (white solid line) as observed by GOES and radio intensity profile (red colored) from BIRS data are shown

and it may not be generated from the leading edge of the CME. Also from the height and time of CME observations at the time of this low frequency metric and DH type II bursts, reveal that CME is the possible event that could produce such bursts⁴. The onset time of metric type II bursts is close to the flare rise time as shown in the Fig. 3b. Generally, the flare rising phase is related to the acceleration phase of the CME in flare-CME associated events. This interpretation suggests that metric type II is due to shocks driven by the CME.

3.2 Low frequency radio burst

The broadband type II feature in the frequency range of ~ 1.5 MHz to 250 kHz between 04:30 UT - 07:30 UT is shown in Fig. 4. The drift rate of the feature is found as 0.115 kHz/s. According to 2-fold LDB model¹⁴, this radio emission might be started around 8 R_o and maximum distance attained at the end of the burst at 250 kHz is ~ 42 R_o . The shock speed for this feature is found using the above density model as 1300 km/s [(42 R_o - 8 R_o)/(3 \times 60 \times 60)]. As listed in LASCO catalogue, the CME was at a distance of ~ 22 R_o during the onset time (04:30 UT) of this broadband feature. Since the CME is fast and energetic, it could produce intense type II bursts of broad band signatures. The intense

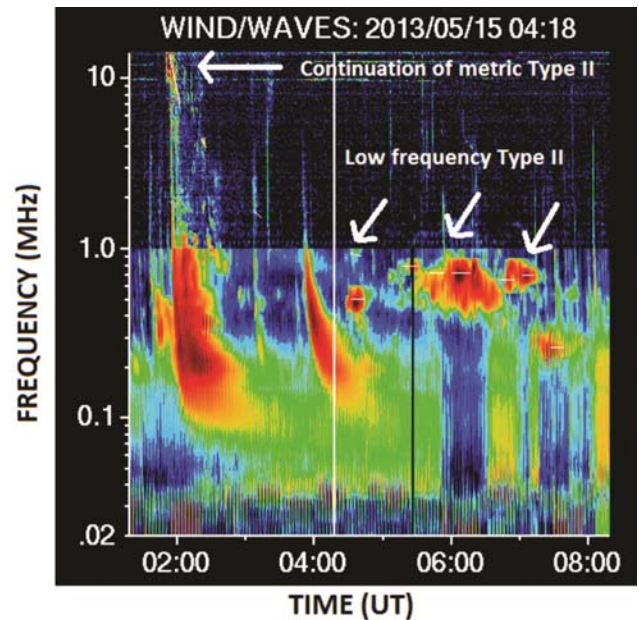


Fig. 4 — DH type II burst recorded by Wind/WAVES on 2013 May 15. The metric continuation type II burst of fundamental component is marked between 14 MHz – 7 MHz from $\sim 01:48$ UT – 02:05 UT. The start and end of low frequency type II bursts are marked between the frequency range 1.5 MHz – 250 kHz from 04:30 UT – 07:30UT. The white lines indicate the centre frequency of the dynamic spectrum

broadband feature is visible clearly in the Wind/WAVES spectrum during 05:30 UT – 06:30 UT and it denotes that the shock strength is greater. This study suggests that the intense broadband feature is due to ICME driven magnetosonic shock in the interplanetary medium²⁰. During the propagation above 8 Ro, the CME is found to be interacted with a high density medium of an ongoing pre CME which ejected from same active region (11748) which may act as high density solar wind structure, where the Alfvén speed (~350 km/s) was below the CME speed (1400 km/s). In that suitable condition on the outside of corona and in the interplanetary medium, Magnetohydrodynamics (MHD) shock waves might have accelerated more electrons. The type II shock speed (1300 km/s) from density model is similar to the CME speed (~1400 km/s) measured using LASCO images. The CME speed is found as 2063 km/s using STEREO-B coronagraph during the low frequency radio emission. The difference in shock speed between using LDB model (1300 km/s) and observed STEREO data (2063 km/s) is mainly due to CME interaction with high density solar wind structure. This kind of event is similar to a slow and fast CME interaction event that it is not necessary to obey the electron density model due to different MHD condition also, density model is valid at normal solar wind condition. This study suggests that the intense broad band radio

feature is mainly due to CME-high density solar wind interaction. The radio feature is shown as a continuum and slow drift type with respect to time and it is mainly associated with MHD shock waves. Some kind of radio features associated with a CME-CME interaction event were reported by Gopalswamy *et al.*⁴ and Shanmugaraju *et al.*²⁰ Figure 5 also indicates that strengthening of shock during the enhancement frequency emission between the height range 8 Ro – 42 Ro. Figure 6 shows the over plot of the type II burst flow at solar wind condition using 2 fold LDB model with the observed centre frequency of the present study. Figure 6 shows the solar wind, magnetic field, Alfvén speed and density profile associated with type II burst using various shock models. The density, magnetic field in Fig. 6 appeared to be similar flow with respect to distance. The Alfvén speed (< 800 km/s) and solar wind speed (< 500 km/s) are found to be lower than that of observed shock speed (2063 km/s) at the height range [8 Ro – 42 Ro]. In this able condition, the non-thermal MHD shocks generated in front of the CME during high density solar wind-CME interaction which was driven by the CME.

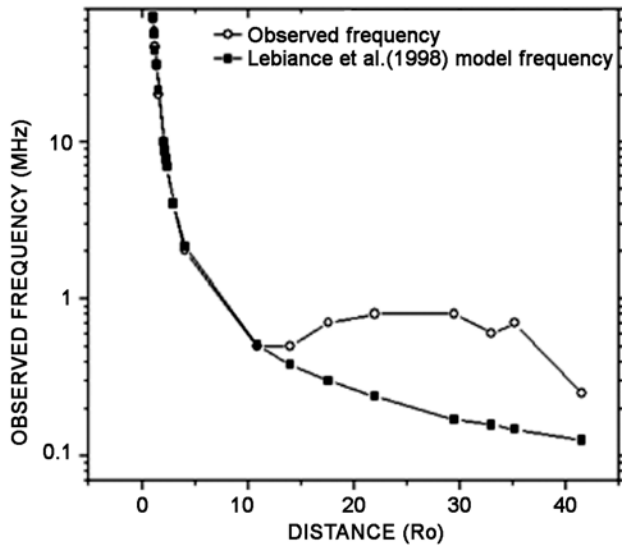


Fig. 5 — Distribution of shock height and centre frequency of the radio signatures are seen in the DH spectrum. The dashed line with points (marked with circle) is drawn for observed centre frequency. The dashed line with points (marked with square) is drawn using the 2 fold Leblanc *et al.*¹⁴ model. The density jump in observed frequency between ~10 Ro – 42 Ro is due to CME interaction

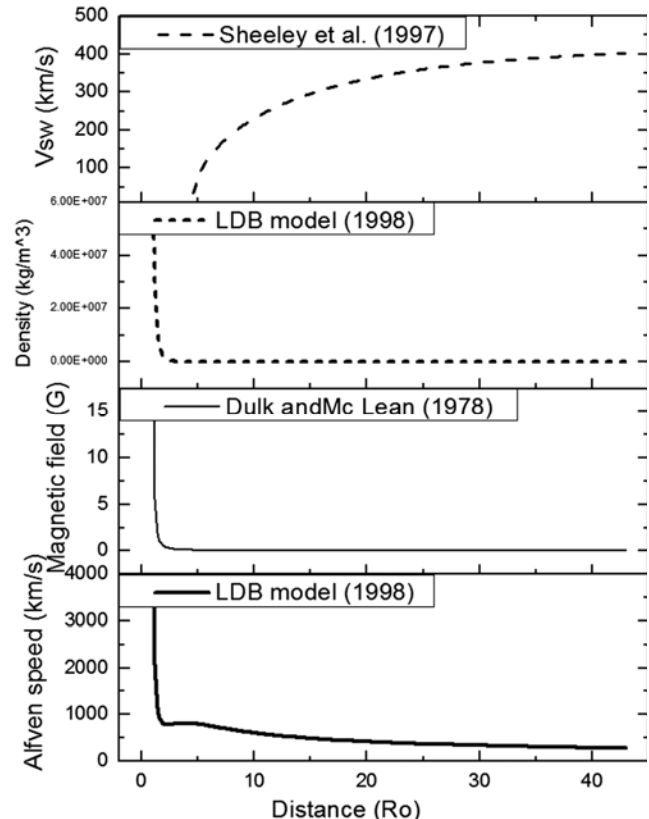


Fig. 6 — The solar wind speed, plasma density, magnetic field and Alfvén speed profile using models show the interplanetary condition during the type II radio emission

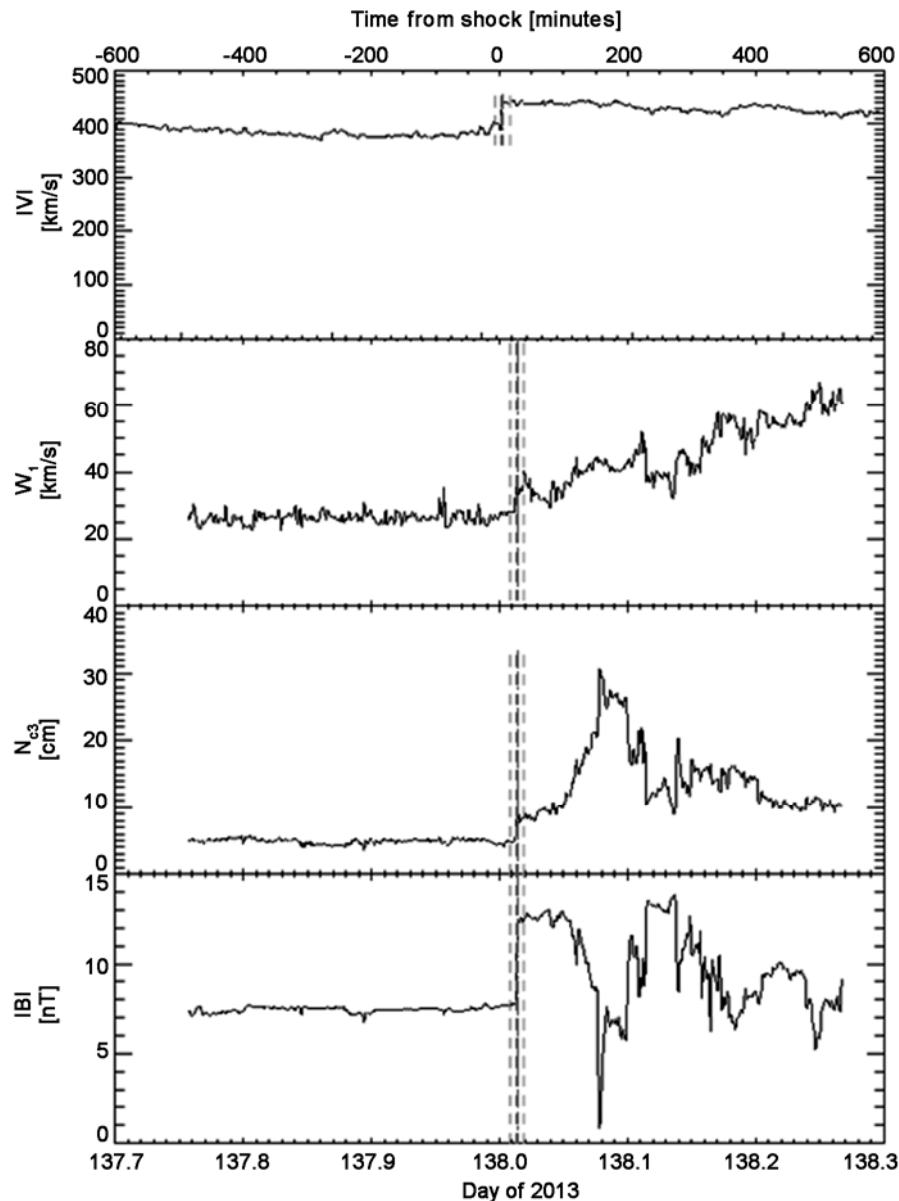


Fig. 7 — IP shock detected by the Wind shock monitor is considered from CFA Wind spacecraft shock data base. The shock arrival at 1AU at 00:19 UT on 18 May 2013 is shown as red line. The transit time of this shock from the Sun to the Earth is found as 71 h

Note that the observed CME speed may have projection correction because it is measured using the sky-plane projected CME images. As suggested by Gopalswamy and Kaiser⁴, the Alfvén speed at 8 R_{\odot} is ~ 350 km/s. Both the shock speed and CME speed were super Alfvénic (>350 km/s) above 8 R_{\odot} . None other activity except this shock was present during that time inside and outside the corona. Generally speaking, from the earlier studies it has been found that CMEs are responsible for DH type II bursts. The present study also suggests that this low frequency type II radio feature between the

range 1.5 MHz – 250 kHz is due to CME driven shock¹.

3.3 Other Associated activities

The CME is also associated with a major SEP event [>10 particle flux unit (pfu)]. The proton emission onset time and peak intensity are listed as 06:35 UT on 15 May 2013 and 42 pfu, respectively. The time delay between DH type II start and SEP start is found to be 287 min. The SEP started at 06:35 UT and that was during the time of DH type II broadband feature (04:30 UT–07:30 UT). The SEP onset time

within the duration of low frequency DH type II suggests that the shocks responsible for low frequency type II burst accelerated higher amount of electrons and protons. Interacting CMEs associated with DH type II radio burst cause solar energetic particles (SEP) as listed by Gopalswamy *et al.*⁴ Interacting CMEs associated with flare and DH type II radio burst are in close association with some proton acceleration as suggested by Shanmugaraju and Prasanna²⁰. This study suggests that CME-CME interaction is the cause for proton acceleration during the broad band enhancement feature.

The IP associated with this CME was also detected by Wind/MFI spacecraft on board. The increase in the solar wind plasma parameters such as magnetic field (B), proton density (n_p) and solar wind speed (V_{sw}) from downstream to upstream suggest that the kind shock is a fast and forward type shock²¹. As shown in Fig. 7, the IP shock was detected at 1AU on 18 May 2013 at 00:19 UT. The transit time of shock from solar corona to 1AU is 71 h. The geomagnetic storm, as measured using Dst index, of the event is noted from the catalogue as -55 nT. The above study suggests that CME is the cause of Type II burst, SEP, IP shock and geomagnetic storm.

4 Conclusions

An intensive flare-CME associated event on 15 May 2013 and the corresponding radio emissions are analyzed using multi-wavelength data from SOHO/LASCO, GOES, STEREO, Culgoora, BIRS and Wind/WAVES etc. The heights of radio emissions are analyzed utilizing the known electron density model¹⁴. The following conclusions are drawn from this study:

(i) The high frequency emission is found in the frequency range 32-7 MHz using BIRS and Wind/WAVES spectrograph (Cane and Ericson, 2005) are found to be generated in the distance range 1.5-2.6 Ro according to 3 fold Saito density model²². The shock height is estimated for the intense broadband frequency range 1.5 MHz - 250 kHz in Wind/WAVES spectrograph using 2 fold Leblanc density model and it corresponds to 8-42 Ro. Both the high and low frequency radio feature is also found to be generated due to CME driven shock¹.

(ii) The low Alfvén speed during the enhancement frequency period and wide enhancement frequency suggest that the strengthening of the shock during that time during the propagation.

Acknowledgement

The authors gratefully acknowledge the data support provided by various online data centres of NOAA and NASA. They would like to thank the Culgoora, BIRS, Wind/WAVES teams for providing the Type II catalogues. The CME catalogue used is provided by the Centre for Solar Physics and Space Weather, The Catholic University of America in cooperation with the Naval Research Laboratory and NASA. They thank Geomagnetic Division of Kyoto University Japan for providing Dst data. They thank Dr P K Manoharan, RAC-TIFR, Ooty and all RAC staff for their support throughout this work.

References

- 1 Gopalswamy N, Rodriguez E A, Yashiro S, Nunes S, Kaiser M L & Howard R A, *J Geophys Res*, 110 (2005) A12.
- 2 Vršnak B, *J Geophys Res*, 106 (2001) 25291.
- 3 Vršnak B, Magdalenic J, Aurass H & Mann G, *Astron Astrophys*, 396 (2002) 673 .
- 4 Gopalswamy N & Kaiser M L, *Adv Space Res*, 29(3) (2002) 307-312.
- 5 Vršnak B & Cliver E W, *Solar Phys*, 253(2008) 215.
- 6 Shanmugaraju A, Moon Y J, Dryer M & Umapathy S, *Solar Phys*, 217 (2003) 301.
- 7 Prakash O, Umapathy S, Shanmugaraju A & Vršnak B, *Solar Phys*, 258 (2009) 105.
- 8 Vasanth V, Umapathy S, Vršnak B & Mahalakshmi M, *Solar Phys*, 273 (2011) 143.
- 9 Lawrence B, Shanmugaraju A & Prasanna Subramanian S, *Indian J Radio Space Phys*, 44 (2015) 113.
- 10 Kahler S W, Reames D V & Sheeley Jr N R, *Astrophys J*, 562 (2001) 558.
- 11 Gopalswamy N, Yashiro S, Akiyama S, Makela P, Xie H, Kaiser M L, Howard R A & Bougeret J L, *Ann Geophys*, 26 (2008) 3033.
- 12 Klein K L, J I Khan, N Vilmer, J M. Delouis & H Aurass, *Astron Astrophys*, 346 (1999) L53.
- 13 Gopalswamy N, Xie H, Makela P & Yashiro S, *et al.*, *Adv Space Res*, 51(11) (2013) 1981.
- 14 Leblanc Y, Dulk G A & Bougeret J L, *Solar Phys*, 183 (1998) 165.
- 15 Yashiro S, Gopalswamy N, Michalek G, St Cyr O C, Plunkett S P, Rich N B & Howard R A, *J Geophys Res*, 109 (2004) 7105.
- 16 Aschwanden M J, *Physics of the Solar Corona. An Introduction*, (Praxis Publishing Ltd., Chichester, UK, and Springer-Verlag Berlin), 2004.
- 17 Cane H V & Erickson W C, *Appl Phys J*, 623 (2005) 1180.
- 18 Dulk G A & McLean D J, *Solar Phys*, 57 (1978) 279.
- 19 Sheeley N R, Jr Wang Y M & Hawley S H *et al.*, *Appl Phys J*, 484 (1997) 472
- 20 Shanmugaraju A, Suresh K & Moon Y J, *Sol Phys*, 351 (2014) 67.
- 21 Heikinmaa K H & Valtonen E, *Ann Geophys*, 23 (2009) 767.
- 22 Saito K, Poland A I & Munro R H, *Solar Phys*, 55 (1977) 121.